Generic Phase Behavior of Branched-Chain Phospholipid Monolayers

Frank Bringezu,[c] Bodo Dobner,[b] and Gerald Brezesinski*[a]

Dedicated to Professor Peter Nuhn on occasion of his 65th birthday

Abstract: Monolayers of chemically modified triple-chain phospholipids have been investigated at the air/water interface using pressure–area isotherms. The condensed phases of the lipids were characterized by grazing incidence X-ray diffraction (GIXD). Increasing chain length corresponds to a temperature effect, which was quantified for different lipids, depending on the head group structure using isotherm (two-dimensional systems) and DSC (three-dimensional systems) measurements. The combination of structure investigations revealed generic phase diagrams, which describe the phase behavior of multiple-chain lipids in two dimensions. For the 1-acyl-2-*O*-alkyl phospholipids, the generic phase diagram exhibits only L_{2d}, LS and LE phases while the exchange of the position of the branched acyl and the non-branched alkyl chains at the glycerol backbone leads to a much richer polymorphism (L_{2h}, L_{2d}, Ov, LS, S, τ, LE). Here we present the first experimental evidence of the unusual τ phase for multiple-chain lipid monolayers. This phase exhibits an undistorted in-plane lattice despite of tilted chains.

Keywords: nano monolayers · structures · phase diagrams · phospholipids · X-ray diffraction

Introduction

Phospholipids as major building blocks of biological membranes have been continuously studied over the last decades using a variety of approaches. Under physiological conditions, they build a liquid crystalline matrix in aqueous dispersions.[1] From a physicochemical point of view, their ability to form various structured mesophases in a self-organizing manner, such as multilayers, non-lamellar phases or monolayers at interfaces is of particular interest.

Langmuir monolayers at the air/liquid interface are excellent model systems for studying ordering in two dimensions. The liquid surface is ideally smooth and many thermodynamical variables can be directly controlled. Additionally, intramonolayer and monolayer-subphase interactions can be easily varied by changing the chemical structure of the amphiphilic molecules or by changing the subphase composition (pH, ions, surface active molecules such as enzymes or proteins). Langmuir monolayers exhibit a rich polymorphism which can be easily investigated by numerous techniques.[1–5] Pressure/area isotherm measurements provide a straightforward physicochemical characterization since molecular area and lateral pressure are directly accessible. At certain temperatures, typical lipids such as single chain fatty acids or double chain phospholipids reveal a gas-analogous phase at very large molecular areas; with compression liquid-expanded (LE) and -condensed (LC) phases can be observed. The first-order phase transition between LE and LC results in a plateau region in the pressure/area isotherms, while kinks indicate higher order transitions between condensed phases. Using X-ray diffraction techniques the structures of different condensed phases have been characterized within Å resolution; this supports the occurrence of the kinks as phase transitions between condensed phases differing in tilt angle, tilt direction, lattice spacings and lattice distortion.[6–9] As expected, it was shown that these structural parameters depend systematically on the chemical nature of the amphiphiles.[10–14]

Moreover, Langmuir monolayers at the air/water interface are very useful model systems for membrane biophysics, since biological membranes can be considered as two weakly coupled monolayers. They are successfully used for studies of chemical and biological reactions at interfaces.[15] In general, model membrane studies with phospholipids can be performed using either lipid extracts from natural sources or synthetic single components. The latter is advantageous for the use of systematic chemical approaches to modify specific parts of the molecules in order to understand the molecular

[a] Dr. G. Brezesinski
Max-Planck-Institute of Colloids and Interfaces
Am Muehlenberg 1, 14476 Golm/Potsdam (Germany)
Fax: (+49) 331-567 9202
E-mail: brezesinski@mpikg-golm.mpg.de

[b] B. Dobner
Institute of Pharmaceutical Chemistry
Martin-Luther-University Halle, 06099 Halle (Germany)

[c] F. Bringezu
Institute of Biophysics and X-ray research
Schmiedlstrasse 6, 8042 Graz (Austria)

  0947-6539/02/0814-3203 $ 17.50+.50/0

interactions involved in the structure formation as well as in structure–function relationships.[16] Therefore, chemically modified lipids have been prepared with variations in the head group and chain regions. Branched-chain lipids are of particular interest in such investigations not only because they are found in nature,[17] but also because they allow systematic studies of general features which determine the structure in model membranes.[12–14, 18–22] For example, branchings in the fatty acid chains have a strong influence on the physicochemical properties of the corresponding phospholipids. Short-chain branchings disturb the lateral packing and shift the main-phase transition temperature to lower values similar to the effect of double bonds, but without the problem of forming lipid oxidation products. The isoprenoid pattern of methyl-branchings in archaebacterial lipids is responsible for the higher stability against proton permeability and also for fluidity of membrane-spanning bipolar lipids.[23]

Long branches in the hydrophobic region have gained our interest because they enable systematic changes in the area requirements of the two parts of amphiphilic molecules that leads to a change in molecular shape and therefore to the appearance of non-lamellar phases.[10, 24]

Detailed studies on homologous series of single-chain fatty acid monolayers elucidated the correlation between chemical structure (e.g. aliphatic chain length) and polymorphism. The phase transition lines of monolayers of fatty acids were matched on a common phase diagram by systematically shifting the temperature axis.[25] For example, a fixed shift of the temperature axis by 5 °C per methylene group is required for chain lengths between C16 and C22. This means, that molecules differing only in the chain length exhibit the same phase sequence but at different temperatures. From these investigations, a generic phase diagram[25, 26] and a detailed thermodynamic and structural correspondence between monolayers formed of molecules with different chain lengths were found. Based on the Landau theory[27] theoretical considerations were applied to describe the phase transitions and the relations between the structures of different phases in terms of coupling of a limited number of order parameters.[28, 29]

Although substantial effort was made in describing the physicochemical parameters and structures of condensed monolayers of chemically modified multiple-chain phospholipids, a more general approach to the relation between chemical structure and monolayer behavior is still missing. The aim of the present study is to provide a generalized description of the monolayer behavior of lipids that have been systematically modified in the head group and chain regions. Based on this analysis, generic phase diagrams of multiple-chain lipids are derived.

Results and Discussion

The chemical structures of the phospholipids used in this study are summarized in Table 1. All triple-chain phospholipids form stable monolayers at the air/water interface in a wide range of temperature. Starting at low temperatures, the lipids exhibit fully condensed isotherms and with increasing temperature, the typical first-order transition from a liquid-expanded (LE) to a condensed phase (LC) appears. The transition pressure (π_C) increases with increasing temperature and the area change (ΔA) involved in the transition decreases.

Figure 1 shows the isotherms for compounds **1** and **2** differing in the length of the branched fatty acid chains. The increase of the chain length (e.g. compound **2** compared with **1**) has the same effect as a decrease in temperature. From the area change ΔA it is possible to derive information about the transition enthalpy ΔH using a modified Clausius–Clapeyron equation.[30] Figure 2 gives the enthalpy (ΔH) and the pressure

Table 1. Chemical structures of the compounds investigated.

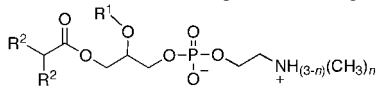

Compound	n	R^1	R^2
1	1	$-C_{16}H_{33}$	$-C_{14}H_{29}$
2	1	$-C_{16}H_{33}$	$-C_{16}H_{33}$
3	2	$-C_{16}H_{33}$	$-C_{14}H_{29}$
4	2	$-C_{16}H_{33}$	$-C_{16}H_{33}$
5	3	$-C_{16}H_{33}$	$-C_{14}H_{33}$

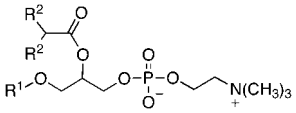

Compound	R^1	R^2
6	$-C_{16}H_{33}$	$-C_{14}H_{29}$
7	$-C_{16}H_{33}$	$-C_{16}H_{33}$

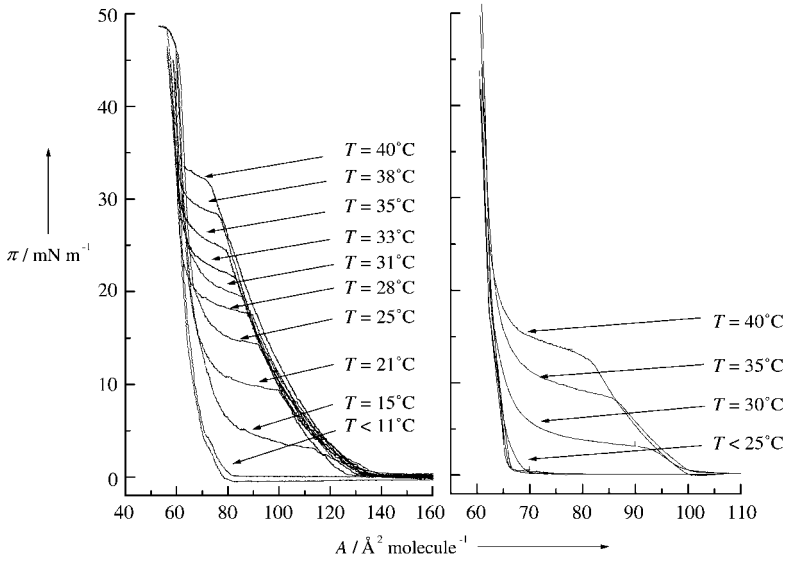

Figure 1. Surface pressure/molecular area isotherms of compounds **1** (left) and **2** (right) at different temperatures as indicated.

0947-6539/02/0814-3204 $ 17.50+.50/0 *Chem. Eur. J.* **2002**, *8*, No. 14

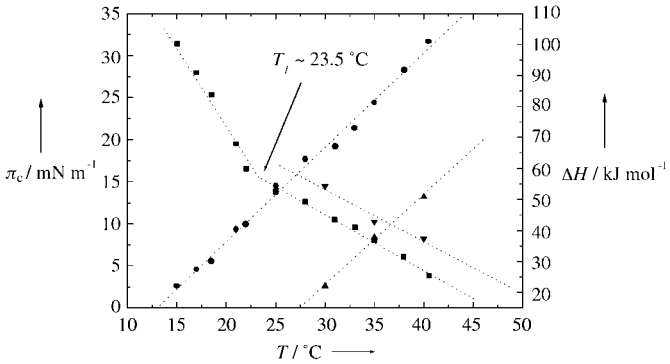

Figure 2. Transition pressure π_C (compound **1**: ●, compound **2**: ▲) and enthalpy ΔH (compound **1**: ■, compound **2**: ▼) of the main transition (LE–LC) of monolayers of compounds **1** and **2** as function of temperature. The extrapolation towards $\pi_C = 0$ gives the onset temperature T_0 of the phase transition, whereas the extrapolation towards $\Delta H = 0$ yields the critical temperature T_C.

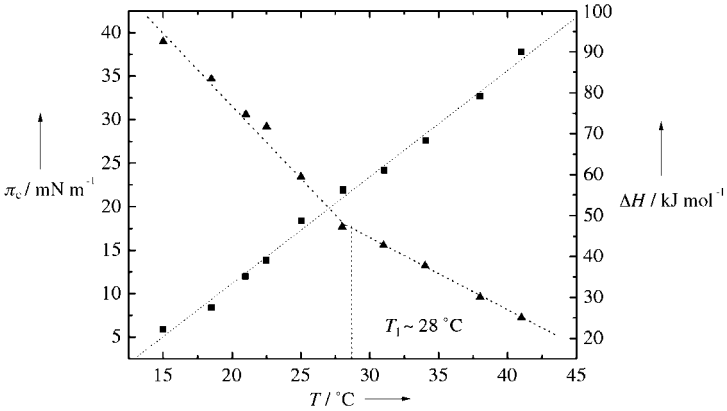

Figure 3. Transition pressure π_C (■) and enthalpy (▼) of the main transition (LE–LC) of compound **3** as function of temperature. The extrapolation to zero π_C gives the onset temperature $T_0 = 11\,^{\circ}C$. At temperatures above 28 °C, the linear extrapolation of ΔH towards zero yields $T_C = 56\,^{\circ}C$.

(π_C) of the main-transition as function of temperature for compounds **1** and **2**. Over a wide range of temperature, both the π_C and the ΔH values are linear functions. The linear extrapolation of the π_C values towards $\pi_C = 0$ gives the onset temperature T_0 of the main-transition: 13 °C for compound **1** and 27 °C for compound **2** (see Table 2). The ΔH versus T function of compound **1** clearly shows a pronounced slope change at a temperature T_1 of ≈23.5 °C. The extrapolation towards $\Delta H = 0$ gives the critical temperature T_C of about 56 °C. Above this temperature, a condensed phase cannot be achieved by compression of the monolayer. Increasing chain length corresponds to a decrease in temperature; therefore, one could expect a shift of T_1 towards higher values. Taking this into account, the estimate of the critical temperature for compound **2** from only three points in the ΔH versus T function is impossible. DSC measurements of lipid/water dispersions in the water-saturated two-phase region ($c_w > 60$ wt %) of compounds **1** and **2** yielded T_m values (Table 2) of 39.3 and 50.6 °C, respectively. It should be noted that the resulting ΔT_m of ≈11 °C is very similar to the difference in the T_0 values ($\Delta T_0 = 14\,^{\circ}C$).

The results for compound **3** including a second methyl unit in the head group region are summarized in Figure 3. From these data T_0 and T_C were determined to be 11 °C and 56 °C, respectively, which indicates only slight changes in the physicochemical parameters caused by the second methyl unit. The ΔH versus T plot also displays the kink found for **1**; however, the temperature T_1 of the kink is shifted towards higher values: 28 °C. The fully condensed monolayers of compound **4** have been investigated by GIXD only at temperatures below 20 °C. Therefore, neither T_0 nor T_c values have been determined. However, in lipid/water dispersions a shift in the T_m values of approximately 13 °C due to increased chain length has been observed: 38.3 and 50.9 °C for compounds **3** and **4**, respectively.

Table 2. Characteristic temperatures of monolayers (T_0: lower limit of the region for the liquid expanded phase; T_C: critical temperature or upper limit of the region for the liquid expanded phase; T_1: temperature of the kink in the $\Delta H = f(T)$ plot) and the data for the main transition from the gel to the liquid crystalline phase of the lipid water dispersions (T_m: transition temperature, ΔH: transition enthalpy) are given for compounds **1**–**7**.

Compound	T_0 [°C]	T_C [°C]	T_1 [°C]	T_m [°C]	ΔH [kJ mol^{-1}]
1	13	56	23.5	39.3	55
2	27	–	–	50.6	58
3	11	56	28	38.3	42
4	–	–	–	50.9	52
5	6	58	23	42.7[18]	41[18]
6	6	58	23	40.5[22]	38[22]
7	23	73	33	53.9	47

The complete exchange of the three hydrogen atoms by methyl units leads to the triple-chain phosphatidylcholines **5**–**7**. For the 1-acyl compound **5**, a critical temperature T_C of 58 °C and a T_0 value of 6 °C was determined. Exchanging the alkyl and the acyl chains does not alter the T_C and T_0 values. However, when the main-transition temperatures (T_m) of lipid/water dispersions are compared, compound **5** shows slightly larger values (**5**: 42.7 °C, **6**: 40.5 °C). Increasing chain length (compound **7**) effects the temperatures more drastically leading to 23 °C and 73 °C for T_0 and T_C, respectively. The difference in T_C amounts to 15 °C and ΔT_0 amounts to 17 °C. The shift in the characteristic temperatures of the monolayers on going from **6** to **7** of about 16 °C is comparable to the difference in the T_m values of the lipid dispersions of approximately 14 °C. It should be noted, that the T_m values of the triple-chain phospholipids depend only very slightly on the head group structure, whereas the T_m values of double-chain phospholipids decrease with increasing degree of head group methylation.[31, 32] This indicates that the head groups have only a small influence on the melting behavior of triple-chain lipid dispersions due to the much larger hydrophobic area. In some cases, this mismatch of the space requirements between hydrophilic and hydrophobic parts of the molecules even leads to a head group interdigitation.[10, 12]

GIXD measurements were performed to elucidate the two-dimensional symmetry of the chain lattices on the Å scale. Figure 4 depicts the contour plots of the diffracted intensities for compound **7** at 15 °C. Starting at low pressures, the monolayer exhibits two low-order diffraction peaks; the degenerate $(1, \pm 1)$ reflection above the horizon and the

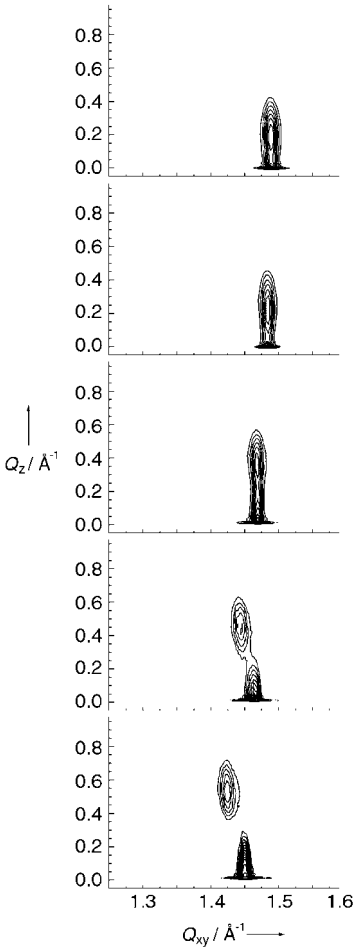

Figure 4. Contour plots of the corrected X-ray intensities as function of the in-plane and out-of-plane scattering vector components Q_{xy} and Q_z for compound **7** obtained at 15 °C and at 2, 14, 34, 40 and 44 mN m^{-1} (from bottom to top).

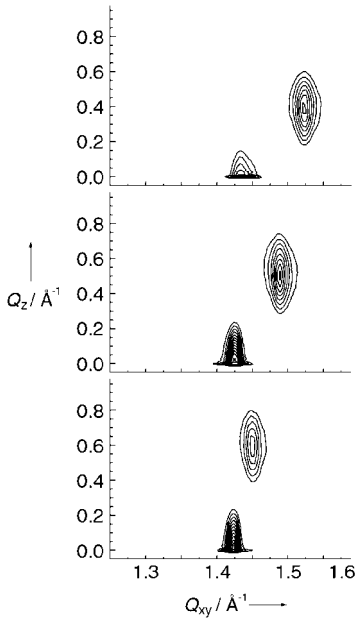

Figure 5. Contour plots of the corrected X-ray intensities versus in-plane and out-of-plane scattering vector components Q_{xy} and Q_z for compound **7** at 5 °C. The results obtained at 1, 20 and 40 mN m^{-1} (from bottom to top) are shown.

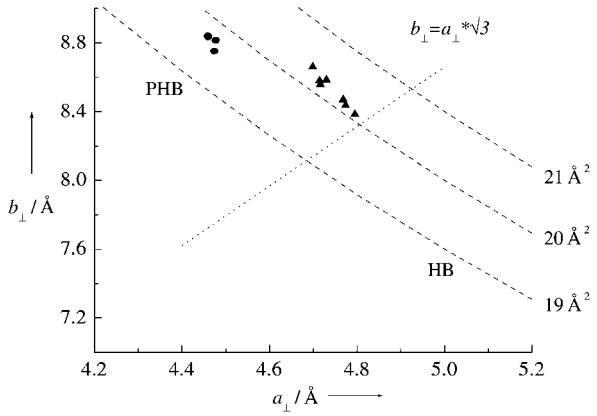

Figure 6. Distribution of unit cell parameters ($a_\perp$, $b_\perp$) in the cross section normal to the chains extracted from the GIXD measurements of compound **7** at 15 °C (▲) and 5 °C (●). The dashed lines correspond to values of constant cross-sectional area per hydrocarbon chain ($A_0 = a_\perp b_\perp/2$). The dotted line gives lattice constants of a hexagonal projected unit cell ($b_\perp = a_\perp\sqrt{3}$). The labels HB and PHB denote the regions characteristic for herringbone and pseudo-herringbone packing according to Kaganer et al.[9]

non-degenerate (0,2) reflection at zero Q_z are indicative of a condensed phase with a centered rectangular chain lattice. The chains are tilted in the direction towards nearest neighbors (NN) along the short axis of the in-plane unit cell. The lattice is distorted from hexagonal packing in NN direction ($Q_{xy}^{n} > Q_{xy}^{d}$), where Q_{xy}^{n} is the maximum position of the non-degenerate peak.[33] With increasing pressure, the degenerate peak moves to larger Q_{xy} values and above 27 mN m^{-1} the Q_{xy} positions of the two diffraction peaks coincide; this indicates hexagonal in-plane packing despite a large tilt angle. Further pressure increase leads to a decrease of the tilt angle although the in-plane packing remains hexagonal. Perpendicular to the chains, the lattice is distorted and the distortion decreases with increasing pressure. At lower temperatures, the lattice is still orthorhombic but the distortion direction is now NNN (next-nearest neighbor) (Figure 5).

The cross-sectional area decreases from 20.3 Å^2 at 15 °C to 19.7 Å^2 at 5 °C. This leads to increased tilt angles at lower temperatures. Figure 6 shows the distribution of unit-cell parameters $a_\perp$ and $b_\perp$ in the cross-section normal to the chains. These parameters are much less influenced by the tilt since they are governed by equilibrium between van der Waals attraction and short-range repulsion as well as the rotational and conformational freedom of the chains at a given temperature.[9] The data points lie on the same large arc as observed for single-chain amphiphiles.[9] As one can see from this plot, the packing at 5 °C is close to a pseudo-herringbone packing (PHB).[34] The PHB motif should have an angle of 40° between the backbones planes of the chains. The projected cell parameters of the PHB arrangement as estimated by Kitaigorodskii[35] are $a_\perp = 4.2$ Å and $b_\perp = 9.0$ Å. The corresponding values of compound **7** are 4.46 and 8.84 Å. The transition to a non-tilted phase was not observed. The GIXD measurements on monolayers of the other compounds show similar diffraction patterns. Two diffraction peaks are observed at low pressures and increasing pressure leads to the

  0947-6539/02/0814-3206 $ 17.50+.50/0 *Chem. Eur. J.* **2002**, *8*, No. 14

phase transition towards the non-tilted phase. Only in the case of compound **6** an NNN tilted phase was observed at 15 °C and low lateral pressure.

Since the condensed isotherms exhibit linear relations between pressure and molecular area: $A_{xy} = K_1 - K_2\pi$, where $A_{xy} = A_0/\cos(t)$ with A_0 as cross-sectional area of the chains and t as chain tilt angle, plotting of $1/\cos(t)$ as a function of π allows the determination of the tilting phase transition pressure π_t by extrapolation towards $1/\cos(t) = 1$. Figure 7 shows an example for a linear extrapolation for compounds **1**, **3** and **5**, which resulted in transition pressures π_t of 11 mN m^{-1} (**1**), 18 mN m^{-1} (**3**) and 19 mN m^{-1} (**5**).

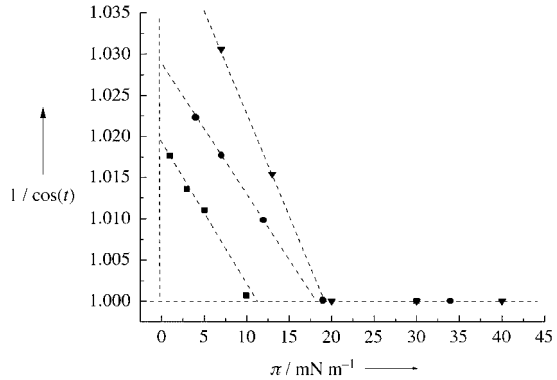

Figure 7. $1/\cos(t)$ as function of the lateral pressure π for compounds **1** (■), **3** (●) and **5** (▼) at 5 °C. The linear extrapolation towards zero tilt angle ($1/\cos(t) = 1$) yields the pressure π_t of the tilting transition.

Comparison of the characteristic temperatures found in the monolayer (T_0, T_C) and bilayer (T_m) measurements shows that the corresponding phospholipids, which differ only in the length of the branched chains, can be compared directly by changing the temperature: 12.5 °C for compounds **1** and **2** as well as **3** and **4** and 14 °C for compounds **6** and **7**. Using this approximation allows the construction of generic phase diagrams for the different branched-chain phospholipids. A generic phase diagram for the branched-chain *glycero*-3-phospho-*N*,*N*-dimethyl-ethanolamines is shown in Figure 8.

In the temperature region investigated, only three different phases (LE, L_{2d} and LS) are observed. The NN-tilted phase L_{2d} is a rotator phase with cross-sectional areas well above 20 Å^2. Increasing pressure leads to the hexatic LS phase with non-tilted molecules. The open symbols represent the extrapolated tilting pressures π_t. The point of intersection between the tilting transition and the main phase transition was taken from the ΔH versus T plots where a change of slope was found. This slope change can now be interpreted as a change in the phase sequence (LE to L_{2d} or LE to LS) which leads to changes in the transition enthalpy derived from isotherm measurements.

A much more complex generic phase diagram for the corresponding branched-chain *glycero*-3-phosphocholines is given in Figure 9. In a small range of temperature and pressure, the NNN-tilted Ov phase has been observed. This phase is characterized by an intensity distribution with two diffraction peaks at non-zero Q_z values with $Q_z^n = 2Q_z^d$. The intersection point between the tilting transition and the main

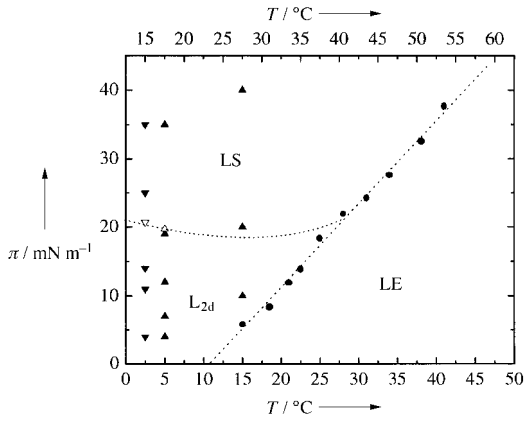

Figure 8. Generic phase diagram for branched chain 1-acyl-2-*O*-hexadecyl-*glycero*-3-phospho-*N*,*N*-dimethylethanolamines derived from experimental data of compounds **3** and **4**. The plot shows the π_C values as function of temperature (●) of compound **3**. The experimental data points from the GIXD measurements of compound **3** (▲) at 15 and 5 °C and compound **4** (▼) at 15 °C are shown. The data for compound **4** are shifted by 12.5 °C towards lower values according to the temperature shift found for the comparison of the T_C, T_0 and T_m values. The top axis shows the temperature of compound **4** while the bottom axis is drawn for compound **3** (see text for details). The phase assignment based on the analysis of the X-ray data is shown in the plot. The L_{2d}–LS phase transition (**3**: △, **4**: ▽) is derived from the extrapolation of $1/\cos(t) \rightarrow 1$.

phase transition was again taken from the ΔH versus T curves. At lower lateral pressures and lower temperatures, the NN tilted rectangular phase L_2 is observed. For symmetry reasons, this phase was subdivided into two phases L_{2d} and L_{2h}, which have disordered and herringbone-ordered backbone planes, respectively.[9] Plotting the signed unit cell distortion $d = (l_1^2 - l_2^2)/(l_1^2 + l_2^2) \cdot \cos 2(\beta - \omega)$, where l_1 and l_2 are the major and minor axes of the ellipse passing through all six nearest neighbors of a hydrocarbon chain, and β and ω are the tilt and distortion azimuths, respectively, as a function of $\sin^2(t)$; a linear relationship is expected according to the Landau theory prediction.[33, 36] This prediction was confirmed by our analysis of the x-ray data. The extrapolation to zero tilt yields a d_0 value, which gives information about the different contributions to the distortion (chain tilt, backbone ordering). The d_0 values of compound **7** are -0.12 at 5 °C and -0.03 at 15 °C and indicate an effect of backbone ordering, whereas the extrapolated d_0 values of compound **6** are zero which suggests that the distortion is induced by tilt only. To compare compounds **6** and **7** directly, we have to shift the measured temperature of compound **7** to lower values by 15 °C in order to get a generic phase diagram of triple-chain PCs. The comparison of the π_C values for compounds **6** and **7** (see Figure 9) strongly supports this assumption. After shifting the π_C versus T function of compound **7** by 15 °C to lower temperatures an almost perfect match is observed. Therefore, the temperatures of the experiments with compound **7** (5 and 15 °C) transfer to 0 and -10 °C for compound **6**. The plot of d_0 versus temperature yields a transition temperature between L_{2h} and L_{2d} of approximately 18 °C (corresponding to 3 °C for compound **6**). Starting from the L_{2h} phase (NN tilt and NNN distortion) at low temperature, increasing pressure should lead to the S phase. This transition occurs at high pressure and was therefore not observed experimentally. At 15 °C (0 °C for

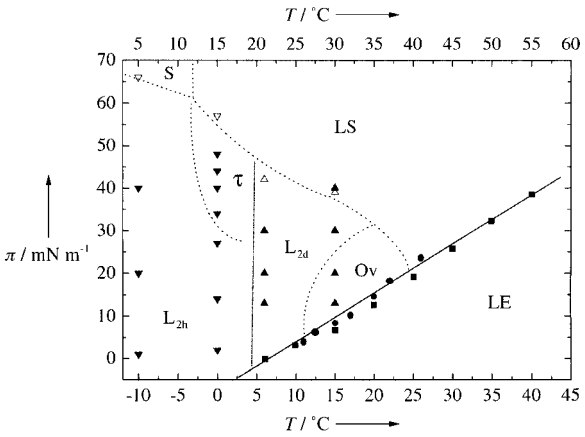

Figure 9. Generic phase diagram for branched chain 1-*O*-hexadecyl-2-acyl-*glycero*-3-phosphocholines derived from experimental data of compounds **6** and **7**. The plot shows the π_C values as function of temperature (**6**: ■, **7**: ●) and the experimentally verified data points for the different phases assigned in the plot. The different symbols represent GIXD data points obtained for compounds **7** (▼), and **6** (▲) at different temperatures. The data for compound **7** are shifted by 15 °C towards lower values according to the temperature shift found for the comparison of the T_C, T_0 and T_m values. The top axis corresponds to compound **7** while the bottom axis is drawn for compound **6**. The phase transition pressures towards the untilted phases (**6**: △, **7**: ▽) are derived from the extrapolation of $1/\cos(t) \rightarrow 1$ (see text for details).

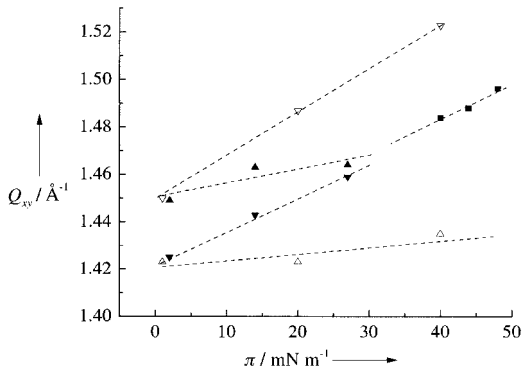

Figure 10. Pressure dependence of the non-degenerate (▼, ▽), the two-fold degenerate (▲, △) and the three-fold degenerate (■) Bragg peak positions of monolayers of compound **7** at 15 °C (filled symbols) and 5 °C (open symbols).

6) and low pressures, the L_{2h} phase exhibits NN distortion. In the case of single-chain amphiphiles, the pressure increase usually leads to a change in distortion from NN to NNN passing through the undistorted state at one defined pressure. In contrast, an unusual behavior was found for compound **7**: increasing pressure leads to an undistorted in-plane lattice that remains undistorted with further pressure increase despite of a change in tilt angle. Such a behavior was previously observed only for methyl eicosanoate monolayers.[37] This phase which possesses a hexagonal unit cell in the horizontal plane (the two peaks have the same Q_{xy} values) even though the molecules are tilted was named τ. It exists at low pressure and higher temperature and has a similar structure to the $L_{2'}$ phase with NNN tilted chains. In contrast, in the case of the triple-chain PC the τ phase originates from the NN tilted L_{2h} phase upon compression.

The pressure dependence of the Q_{xy} values of compound **7** at 15 and 5 °C is shown in Figure 10. From this plot, the linear compressibility along each diffraction vector can be determined as $\chi_{hk} = (dQ_{hk}/d\pi)/Q_{hk}$.[38] The two peaks of the L_{2h} phase show rather different responses to the applied pressure: the position of the non-degenerate (0,2) peak is changed only marginally while the compressibility in the direction of the degenerate $(1, \pm 1)$ reflection is much larger. Increasing temperature leads to small increase of the compressibility perpendicular to the tilt direction (0.31 mN^{-1} at 5 °C and 0.59 mN^{-1} at 15 °C) whereas the compressibility in tilt direction decreases from 1.87 mN^{-1} at 5 °C to 1.36 mN^{-1} at 15 °C. In the undistorted τ phase, the compressibility is isotropic and slightly larger than observed in the L_{2h} phase in tilt direction. Since the τ phase exhibits an undistorted in-plane lattice, a transition to the hexatic LS phase should be expected on increasing pressure.

Conclusion

The present study of multiple-chain phospholipids was focused on systematic changes of the monolayer properties depending on both the chemical structure of the head group region and the modifications in the hydrophobic core of the amphiphiles. The physicochemical characterization performed in isotherm and DSC studies demonstrated that increasing chain length corresponds to decreasing temperature. To quantify the temperature effect, a detailed analysis yielded ΔT values for different lipids depending on the head group structure. Using these ΔT values we were able to obtain generic phase diagrams for triple-chain *glycero*-3-phospho-*N*,*N*-dimethylethanolamines and *glycero*-3-phosphocholines. For the *glycero*-3-phospho-*N*,*N*-dimethylethanolamines, the generic phase diagram exhibits only the phases L_{2d}, LS and LE in the temperature region investigated. The corresponding PC shows a similar phase behavior. Exchanging the position of the branched acyl and the non-branched alkyl chains at the glycerol backbone leads to a much richer polymorphism. In this case, the NNN-tilted Ov phase was observed at higher temperatures. The NN tilted L_2 phase was divided into L_{2h} and L_{2d} using the extrapolated d_0 values (distortion at zero tilt) as predicted by theory. Additionally, increasing pressure at medium temperatures leads to a transition from the L_{2h} to a phase exhibiting zero distortion despite of tilt. These results are the second experimental evidence for such an unusual behavior (τ phase) previously reported for single-chain amphiphiles.

Experimental Section

The branched-chain fatty acids were prepared by alkylation of methyl malonic acid ester with long-chain alkylhalogenides.[39] The structure of the fatty acids was confirmed by mass spectrometry. The purity was checked by gas chromatography of the methyl esters. The melting points of the fatty acids were found to be in agreement with the literature data.[40, 41] The acylation of 1-*O*-benzyl-2-*O*-hexadecyl-glycerol in presence of 4,4′-dimethylaminopyridine as a catalyst yielded the corresponding racemic 1-*O*-benzyl-2-*O*-hexadecyl-3-acyl-glycerols.[42] From these derivatives, the benzyl protecting group was removed and the resulting primary hydroxy function was phosphorylated using 2-bromoethyl-phosphoric acid dichlor-

  0947-6539/02/0814-3208 $ 17.50+.50/0 *Chem. Eur. J.* **2002**, *8*, No. 14

ide. Finally, the resulting bromo esters were converted to the corresponding 1-acyl-2-*O*-alkyl-*glycero*-phosphoethanolamines and their *N*-methylated analogues using *N*-monomethylamine, *N*,*N*-dimethylamine and trimethylamine in ethanol at room temperature, respectively. The final products have been purified by column chromatography using methanol/chloroform/water/ammonia gradients. For characterization and purity check mass spectrometry, high performance liquid chromatography and microanalysis were applied. Selected analytical data are given below:

***rac*-1(2-Tetradecylhexadecanoyl)-2-*O*-hexadecyl-*glycero*-3-phospho-*N*-monomethyl-ethanolamine (1)**: 1(2C_{14}-16:0)-2H-PE(Me); $C_{52}H_{106}N_1O_7P_1$; $M = 888.4\ g\,mol^{-1}$; MS: *m*/*z*: 888.9 $[M]^+$, 910.9 $[M+Na]^+$; m.p. 89–90 °C; elemental analysis calcd (%) for: C 70.30, H 12.03, N 1.58; found: C 70.05, H 11.87, N 1.62.

***rac*-1(2-Hexadecyloctadecanoyl)-2-*O*-hexadecyl-*glycero*-3-phospho-*N*-monomethylethanolamine (2)**: 1(2C_{16}-18:0)-2H-PE(Me); $C_{56}H_{114}N_1O_7P_1$; $M = 944.5\ g\,mol^{-1}$; MS: *m*/*z*: 944.9 $[M]^+$, 966.6 $[M+Na]^+$; m.p. 78–80 °C; elemental analysis calcd (%) for: C 71.21, H 11.86, N 1.48; found: C 71.01, H 12.04, N 1.44.

***rac*-1(2-Tetradecylhexadecanoyl)-2-*O*-hexadecyl-*glycero*-3-phospho-*N*,*N*-dimethyl-ethanolamine (3)**: 1(2C_{14}-16:0)-2H-PE(Me)$_2$; $C_{53}H_{108}N_1O_7P_1$; $M = 902.4\ g\,mol^{-1}$; MS: *m*/*z*: 902.6 $[M]^+$, 925.3 $[M+Na]^+$; m.p. 93–94 °C; elemental analysis calcd (%) for: C 70.52, H 12.06, N 1.55; found: C 69.98, H 12.18, N 1.61.

***rac*-1(2-Hexadecyloctadecanoyl)-2-*O*-hexadecyl-*glycero*-3-phospho-*N*,*N*-dimethyl-ethanolamine (4)**: 1(2C_{16}-18:0)-2H-PE(Me)$_2$; $C_{57}H_{116}N_1O_7P_1$; $M = 958.5\ g\,mol^{-1}$; MS: *m*/*z*: 958.2 $[M]^+$; m.p. 106.5–107 °C; elemental analysis calcd (%) for: C 71.73, H 12.20, N 1.46; found: C 70.83, H 12.04, N 1.42.

***rac*-1-(2-Tetradecylpalmitoyl)-2-*O*-hexadecyl-*glycero*-3-phosphocholine (5)**: 1(2C_{14}-16:0)-2H-PC; $C_{54}H_{110}N_1O_7P_1 \times H_2O$; $M = 934.4\ g\,mol^{-1}$; MS: *m*/*z*: 957 $[M+Na]^+$; elemental analysis calcd (%) for: C 69.41, H 11.86, N 1.49; found: C 69.04, H 11.54, N 1.60.

***rac*-1-*O*-Hexadecyl-2-(2-tetradecylhexadecanoyl)-*glycero*-3-phosphocholine (6)**: 1H-2(2C_{14}-16:0)-PC; $C_{54}H_{110}N_1O_7P_1 \times H_2O$; $M = 934.4\ g\,mol^{-1}$; elemental analysis calcd (%) for: P 3.31; found: P 3.09 (for additional analytical data see [22]).

***rac*-1-*O*-Hexadecyl-2-(2-hexadecyloctadecanoyl)-*glycero*-3-phosphocholine (7)**: 1H-2(2C_{16}-18:0)-PC; $C_{58}H_{118}N_1O_7P_1 \times H_2O$; $M = 990.5\ g\,mol^{-1}$; MS: *m*/*z*: 973.1 $[M]^+$; elemental analysis calcd (%) for: P 3.18; found: P 3.12.

The thermotropic phase behavior in the water-saturated two-phase region (>60 wt% water) was characterized by differential scanning calorimetry (DSC) using a DSC-2 (Perkin–Elmer, Norfolk, CT). For sample preparation, all lipids were dried under vacuo in an oven for 2 h at 50 °C before weighing. The samples (3–5 mg) were transferred into aluminum pans and mixed with water before closing. Multilamellar dispersions were formed during the equilibration above the main-transition temperature (T_m) for 1 h. An empty pan was used as reference. The data were recorded through an interface to a PC. After polynomial baseline fit, the main-transition enthalpies and temperatures have been determined.[43]

The monolayers were spread from a 1 mM p.a. grade chloroform solution onto an ultra-pure water subphase (Millipore, 18 MΩ cm). The pressure/area isotherms were recorded with a Wilhelmy film balance (R&K, Berlin). Grazing incidence X-ray diffraction (GIXD) measurements were performed on pure water as subphase using the liquid surface diffractometer (beamline BW1) at HASYLAB, DESY, Hamburg (Germany). The synchrotron beam was made monochromatic by a Beryllium (002) crystal. Experiments were performed at an angle of incidence of $0.85 \times \alpha_c$ (α_c is the critical angle for total external reflection). A linear position sensitive detector (PSD) (OED-100-M, Braun, Garching, Germany) with a vertical acceptance $0 < Q_z < 1.27\ Å^{-1}$ was used for recording the diffracted intensity as a function of both the vertical (Q_z) and the horizontal (Q_{xy}) scattering vector components. The horizontal resolution of $0.008\ Å^{-1}$ was determined by a Soller collimator mounted in front of the PSD. The analysis of the in-plane diffraction data yields lattice spacings according to $d_{hk} = 2\pi/Q_{xy}^{hk}$. From the in-plane and out-of-plane peak positions it is possible to derive information about the tilt angle and the tilt direction. For more information on the principles of GIXD for the study of two-dimensional condensed films at the air/liquid interface, we kindly refer to detailed reviews published recently.[7–9]

Acknowledgement

We gratefully acknowledge beamtime at HASYLAB, DESY (Hamburg, Germany) and Dr. K. Kjaer for help with the beamline setup and fruitful discussions. Dr. B. Rattay (Martin-Luther-University Halle, Germany) is acknowledged for providing *rac*-1-*O*-hexadecyl-2-(2-tetradecylhexadecanoyl)-*glycero*-3-phosphocholine (**6**), Ms. B. Elsner for helpful assistance and Dr. V. M. Kaganer for discussions on phase diagrams. F.B. is grateful for financial support from the Deutsche Forschungsgemeinschaft (Emmy-Noether-Program grant: BR 1826/2-1).

[1] D. M. Small, *The physical chemistry of lipids*, *Vol. 4*, Plenum Press, New York, **1986**.
[2] R. M. Epand, *Biochim. Biophys. Acta Rev. Biomembr.* **1998**, *10*, 353–368.
[3] D. Möbius, H. Möhwald, *Adv. Mater.* **1991**, *3*, 19–24.
[4] H. McConnell, *Annu. Rev. Phys. Chem.* **1991**, *42*, 171–195.
[5] R. N. A. H. Lewis, D. A. Mannock, R. N. McElhaney, *Membrane lipid molecular structure and polymorphism* in "Lipid Polymorphism and Membrane Properties" (R. M. Epand), *Curr. Top. Membr. Vol. 44*, Academic Press, San Diego, **1997**, pp. 25–102.
[6] J. Als-Nielsen, H. Möhwald in *Handbook of Synchrotron Radiation*, *Vol. 4*, Elsevier, Amsterdam, **1991**, pp. 1–53.
[7] "Synchrotron X-ray Scattering Studies of Langmuir Films": J. Als-Nielsen, D. Jaquemain, K. Kjaer, M. Lahav, F. Levellier, L. Leiserowitz, *Phys. Rep.* **1994**, *246*, 251–313.
[8] D. Jacquemain, F. Leveiller, S. Weinbach, M. Lahav, L. Leiserowitz, K. Kjaer, J. Als-Nielsen, *J. Am. Chem. Soc.* **1991**, *113*, 7684–7681.
[9] V. M. Kaganer, H. Möhwald, P. Dutta, *Rev. Mod. Phys.* **1999**, *71*, 779–819.
[10] F. Bringezu, G. Rapp, B. Dobner, P. Nuhn, G. Brezesinski, *Phys. Chem. Chem. Phys.* **2000**, *2*, 4509–4514.
[11] F. Bringezu, G. Brezesinski, P. Nuhn, H. Möhwald, *Thin Solid Films* **1998**, *329*, 28–32.
[12] F. Bringezu, G. Brezesinski, *Colloid Surface A* **2001**, *183*, 391–401.
[13] F. Bringezu, G. Brezesinski, H. Möhwald, *Chem. Phys. Lipids* **1998**, *94*, 251–260.
[14] R. N. Lewis, R. N. McElhaney, P. E. Harper, D. C. Turner, S. M. Gruner, *Biophys. J.* **1994**, *66*, 1088–1103.
[15] U. Dahmen-Levison, G. Brezesinski, H. Möhwald, J. Jakob, P. Nuhn, *Angew Chem.* **2000**, *112*, 2889–2892; *Angew Chem. Int. Ed.* **2000**, *39*, 2775–2778.
[16] A. G. Lee, K. A. Dalton, R. C. Duggleby, J. M. East, A. P. Starling, *Bioscience Rep.* **1995**, *15*, 289–298.
[17] P. Nuhn, *Fett-Lipid* **1996**, *98*, 335–338.
[18] G. Brezesinski, B. Dobner, H. D. Dörfler, M. Fischer, S. Haas, P. Nuhn, *Chem. Phys. Lip.* **1987**, *43*, 257–264.
[19] G. Brezesinski, G. Förster, W. Rettig, *Makromol. Chem. Makromol. Sym.* **1991**, *46*, 47–54.
[20] G. Brezesinski, B. Dobner, B. Elsner, H. Möhwald, *Pharmazie* **1997**, *52*, 703–706.
[21] F. M. Menger, M. G. Wood, Q. Z. Zhou, H. P. Hopkins, J. Fumero, *J. Am. Chem. Soc.* **1988**, *110*, 6804–6810.
[22] B. Rattay, G. Brezesinski, B. Dobner, G. Förster, P. Nuhn, *Chem. Phys. Lipids* **1995**, *75*, 81–91.
[23] V. Braach-Maksvytis, B. Raguse, *J. Am. Chem. Soc.* **2000**, *122*, 9544–9545.
[24] P. Nuhn, G. Brezesinski, B. Dobner, G. Förster, M. Gutheil, H. D. Dörfler, *Chem. Phys. Lipids* **1986**, *39*, 221–236.
[25] A. M. Bibo, I. R. Peterson, *Adv. Mater.* **1990**, *2*, 309–311.
[26] A. M. Bibo, C. M. Knobler, I. R. Peterson, *J. Phys. Chem.* **1991**, *95*, 5591–5599.
[27] L. D. Landau, E. M. Lifshits in *Statistical Physics*, *Part 1*, Pergamon Press, Oxford, **1980**.
[28] V. M. Kaganer, E. B. Loginov, *Phys. Rev. Lett.* **1993**, *71*, 2599–2602.
[29] V. M. Kaganer, V. L. Indenbom, *J. Phys. II* **1993**, *3*, 813–827.
[30] O. Albrecht, H. Gruhler, E. Sackmann, *J. Phys.* **1978**, *39*, 301.
[31] D. J. Vaughan, K. M. Keough, *FEBS Lett.* **1974**, *47*, 158–161.
[32] S. Mulukutla, G. G. Shipley, *Biochemistry* **1984**, *23*, 2514–2519.
[33] V. M. Kaganer, E. B. Loginov, *Phys. Rev. E* **1995**, *51*, 2237–2249.

  0947-6539/02/0814-3209 $ 17.50+.50/0

[34] I. Kuzmenko, V. M. Kaganer, L. Leiserowitz, *Langmuir* **1998**, *14*, 3882 – 3888.
[35] A. I. Kitaigorodski, *Organic Chemical Crystalography*, Consultants Bureau, New York, **1961**.
[36] L. D. Landau, E. M. Lifshits, *Statistical Physics*, *Part 1*, Pergamon Press, Oxford, **1980**.
[37] W. J. Forster, M. C. Shih, P. S. Pershan, *J. Chem. Phys.* **1996**, *105*, 3305 – 3315.
[38] C. Fradin, J. Daillant, A. Braslau, D. Luzet, M. Alba, M. Goldmann, *Eur. Phys. J. B* **1998**, *1*, 57 – 69.
[39] G. Weitzel, J. Wojahn, *Hoppe-Seylers Z. Physiol. Chem.* **1950**, *285*, 221 – 229.
[40] M. S. Joy, R. Adams, W. M. Stanley, *J. Am. Chem. Soc.* **1951**, *73*, 1261 – 1266.
[41] F. L. Breusch, E. Ulusoy, *Chem. Ber.* **1953**, *86*, 688 – 692.
[42] Z. Selinger, Y. Lapidot, *J. Lipid Res.* **1996**, *22*, 293 – 295.
[43] H. D. Dörfler, G. Brezesinski, *Colloid Polym. Sci.* **1983**, *261*, 434 – 440.

Received: December 20, 2001 [F3752]

  0947-6539/02/0814-3210 $ 17.50+.50/0